ICAS 2016
30th Congress of the International Council of the Aeronautical Sciences
DCC, Daejeon, Korea ; September 25-30, 2016

INTEGRATED CONCEPTUAL DESIGN METHOD CONSIDERING ADVANCED AIRCRAFT SYSTEMS AND AIRCRAFT TRAJECTORY

Takashi Chiba* and Kenichi Rinoie*
***The University of Tokyo, Tokyo, 113-8656, Japan**

Keywords: *aircraft conceptual design, aircraft trajectory, secondary power system, laminar flow control*

Abstract

In order to realize a more fuel-efficient aircraft, new aircraft systems such as More Electric System (MES) or Laminar Flow Control (LFC) have been attracting attention. Therefore, it is important to take into account the effect of these systems in conceptual design. In this paper, we present the aircraft conceptual design method considering the aircraft trajectory and the secondary power systems. We apply this method to the design problem of heavy aircraft and examine how the advanced aircraft systems affect the design results. It was indicated that the detailed effects of MES and LFC during the climb, cruise and descent phases can be considered by taking the aircraft trajectory into account. Although the present aircraft system models are based on theoretical and semi-empirical models, the present integrated conceptual design method enables the effects of the advanced aircraft systems on the aircraft specifications to be discussed.

Nomenclature

L/D	:	Lift-to-drag ratio
$\dot{m}_{bleed}$	:	Bleed air flow
PWX	:	Power off-take
S		Wing area
sfc	:	Specific fuel consumption
S_h		Horizontal tail area
T		Engine thrust
T_{TO}	:	Maximum take-off thrust
W_F	:	Fuel weight
W_{OE}	:	Operating empty weight
W_{sys}	:	System weight
W_{TO}	:	Maximum take-off weight

(Nomenclatures used only in the individual section are defined in each corresponding section.)

1 Introduction

Recently, the reduction of fuel consumption and CO_2 are required because of the increase in the price of fuel as well as environmental issues. To satisfy such demands, various new technologies are being discussed, and some have already been introduced. More Electric Systems (MES) and Laminar Flow Controls (LFC) have been attracting attention. MES uses more electrical systems instead of a conventional bleed system. LFC will have a high ability to improve the aerodynamic performance by reducing the friction drag on the wing. These systems affect the aircraft performance; therefore, it is important to consider their effects in the conceptual design.

In the past research [1], a design method considering a secondary power system was proposed. Moreover in [2], [3] and [4], the effect of MES or LFC on the conceptual design was considered. This method is based on [5] and [6], and the fuel weight fraction method is used in the fuel weight estimation. This method uses the Breguet equation and empirical data of exiting aircraft to estimate the fuel weight. However, since this method uses the representative value when the aircraft consumes 40% of the fuel weight, it is difficult to estimate the effect of

systems during climb, cruise and descent. Therefore, in order to cope with a variety of secondary power systems, which is expected for future introduction, we consider the aircraft trajectory. In references [7] and [8], the effect of the secondary power system was estimated using the aircraft trajectory calculation.

The purpose of this paper is to construct a conceptual design method considering trajectory by using an aircraft dynamic model. Moreover, we apply the MES and LFC to the proposed method and consider the effect of these advanced aircraft systems on the conceptual design results.

2 Trajectory Calculation

In this chapter, the aircraft dynamic model and drag estimation model for the aircraft trajectory calculation are introduced.

2.1 Aircraft Dynamic Model

In the aircraft trajectory calculation, the aircraft is expressed by a six-degrees-of-freedom (DOF) or a three-degrees-of-freedom model [7][8]. The 6DOF model considers both the translational and rotational motion, and it is possible to calculate the complex trajectory. However, in many cases, the 3DOF point-mass model is used in the commercial aircraft trajectory calculation. This is because commercial aircraft conduct very small rotational and sideslip motions during operation. In this paper, we use the 3DOF point-mass model, shown in Eq. (2.1). For simplification, the Earth's roundness, rotation and wind effect are ignored:

$$\begin{aligned} m\dot{V} &= T - D - mg\sin\gamma \\ mV\dot{\gamma} &= L\cos\phi - mg\cos\gamma \\ mV\dot{\psi} &= L\sin\phi/\cos\gamma \\ \dot{m} &= -sfcT \\ \dot{x} &= V\cos\psi\cos\gamma \\ \dot{y} &= V\sin\psi\cos\gamma \\ \dot{h} &= V\sin\gamma \end{aligned} \qquad (2.1)$$

where

D	:	Drag
g		Gravity acceleration
h	:	Altitude
L		Lift
m	:	Aircraft mass
V	:	Velocity
W		Weight
x, y		Aircraft position
γ	:	Flight pass angle
ψ	:	Heading angle
ϕ	:	Roll angle

In Eq. (2.1), the control variables are thrust T, flight path angle γ and roll angle ϕ. Since two-dimensional motions are expected in this paper, roll angle is not considered. Thrust is calculated as the power between thrust and drag equal to the increase rate of the kinetic and potential energy as Eq. (2.2). Flight path angle is calculated as Eq. (2.3).

$$(T - D)V = mg \cdot \frac{dh}{dt} + mV \cdot \frac{V}{dt} \qquad (2.2)$$

$$\gamma = \sin^{-1}\left(\frac{dh}{V} \cdot dt\right) \qquad (2.3)$$

2.2 Optimum Cruise Altitude

In the cruise phase of commercial aircraft, the aircraft is expected to fly at an altitude which can improve the flight distance per unit of fuel. This altitude is called the Optimum Cruise Altitude (OCA) [9]. In this section, the method to calculate the OCA is explained and results applied to the conceptual design are shown.

2.2.1 Calculation method of Optimum Cruise Altitude

The distance that the aircraft flies per unit of time is calculated by Eq. (2.4).

$$dR = Vdt \qquad (2.4)$$

The weight change per unit of time is calculated as follows:

$$dW = -sfcTdt \qquad (2.5)$$

From Eqs. (2.4) and (2.5), the distance per unit of fuel is expressed as follows:

$$r = \frac{dR}{(-dW)} = \frac{V}{sfcT} = \frac{V}{Fuel\ Flow} \qquad (2.6)$$

where, r is called specific range, which represents the flight efficiency of the aircraft. OCA is obtained by calculating the altitude numerically which makes the specific range its maximum.

2.2.2 Step Climb

During the cruise phase of an actual commercial aircraft, for the reason of air traffic control and passenger comfort, the aircraft does not climb continuously during the cruise. Therefore, commercial aircraft usually conduct a step climb. The initial cruise altitude is set higher than the optimum altitude, and if the optimum altitude becomes higher than the cruise altitude, the aircraft climbs up step-by-step.

2.2.3 Application to the Conceptual Design

In this section, we explain the design results obtained by the method described in Chapter 6 to consider the effect of the OCA upon the design results. For comparison, three trajectories are selected as cruise altitudes. They are the altitude which follows the OCA, constant altitude and step climb. The existing aircraft is B777-200 [10] and the airframe configurations, such as the tail area, are fixed as existing ones.

Figures 2.1 and 2.2 show the aircraft trajectory and specific range during cruise. Figure 2.2 shows that the specific ranges r of OCA and step climb are almost the same and that they are higher than that of a constant-altitude flight. Table 2.1 shows the weight of the designed aircraft, W_{TO}, W_{OE} and W_F. From Table 2.1, the aircraft which follows the OCA becomes the lightest. In the step climb, W_{TO} is slightly heavier than that of the OCA. However, in the constant altitude, the fuel weight, W_F, is about 2,000 lbs heavier than the others.

From the above results, it is possible to obtain near-optimal results when the step climb is selected during the cruise. Therefore, we select the step climb to simulate the actual flight.

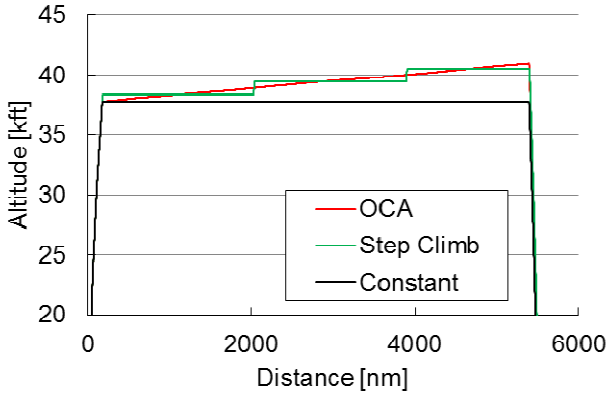

Figure 2.1 Aircraft Trajectory

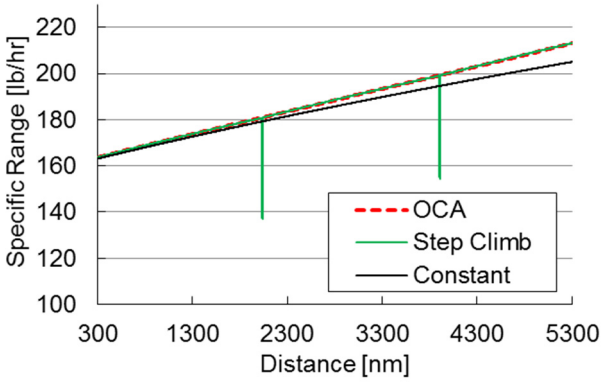

Figure 2.2 Specific Range during Cruise

Table 2.1 Results of W_{TO}, W_{OE} and W_F

	OCA	Step Climb	Constant
W_{TO}[lb]	557,000	558,000	561,000
W_{OE}[lb]	293,000	293,000	293,000
W_F[lb]	205,000	205,000	207,000

3. Aircraft Secondary Power System

The necessary power for the aircraft operation is generated by engines. The secondary power systems shown in Figure 3.1 are driven by the bleed air (Bleed) and power off-take (PWX) from the engines. In this chapter, the estimation method proposed in [2] and [3] is summarized. Moreover, re-modeling of the necessary power for the environmental control system (ECS) is described.

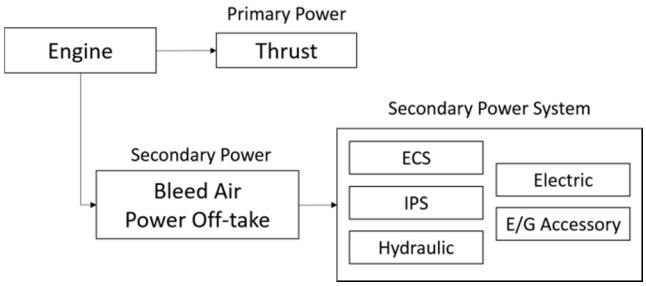

Figure 3.1 Overview of Secondary Power System

3.1 Estimation Method of Secondary Power Systems

In this section, we describe the estimation method of the necessary power of the secondary power systems and the role of each system.

3.1.1 Environmental Control System (ECS)

The ECS keeps the cockpit and cabin comfortable through pressurization, ventilation and temperature control. The necessary bleed air flow $\dot{m}_{bleed}$[kg/s] is calculated in Eq. (3.1) based on FAR part 25§831 [2][3].

$$\dot{m}_{bleed} = 4.158 \cdot 10^{-3} \cdot N_{PAX} \quad (3.1)$$

where N_{pax} is the number of passengers.

The bleed air extracted from the engine is cooled by a pre-cooling machine and a heat exchanger. The cooling air is bled from the ambient air as ram air. Therefore, the ram air causes the drag increase. The drag due to the ram air is called ram drag and is shown in Eq. (3.2).

$$D_{ram} = V \cdot \dot{m}_{ram} - V_{out} \cdot \dot{m}_{out} \quad (3.2)$$

where V_{out} exhaust velocity, $\dot{m}_{ram}$ mass flow rate of the ram air and $\dot{m}_{out}$ exhaust mass flow rate. In this paper, it was assumed that the exhaust flow decelerated enough so that we could neglect the latter term. Thus, the ram drag is estimated as follows

$$D_{ram} = V \cdot \dot{m}_{ram} \quad (3.3)$$

Refinement of the estimation method for ECS

It is known that ECS has the highest influence for the engine specific fuel consumption. Necessary power of the ECS is considered to vary depending on the altitude and the external environment that can be included from the aircraft trajectory considerations. However, the conventional estimation method described above is a simplified one. Therefore, to take into account the trajectory, a more detailed modeling is necessary. In this paper, we consider the energy balance equation to calculate the necessary power of ECS based on the method in [8].

According to [8], bleed air flow for ECS is calculated by Eq. (3.4).

$$\dot{m}_{bleed} c_p (T_i - T_e) - UA(T_c - T_s) + H_s + H_p + H_e = 0 \quad (3.4)$$

where

c_p: Specific heat at constant pressure [J/K]
U: Thermal conductivity of the body [(W/(m^2 · K))]
A: Wall area of the cabin [m^2]
T_i: Inlet temperature [K]
T_e: Exit temperature [K]
T_c: Cabin temperature [K]
T_s: Outside wall temperature [K]
H_s: Heat load of sunlight [W]
H_p: Heat load of passengers and crew [W]
H_e: Heat load of electrical equipment [W]

From [8], the inlet temperature is fixed as 275 K, the exit temperature is equal to the outside temperature, the cabin temperature is fixed as 295 K, and the outside wall temperature is equal to total temperature. From [11], thermal conductivity of the body surface is $U = 2.5$[W/m^{2}K]. The heat load of the passengers and crew is calculated as 70 W per passenger.

In this paper, we use this model as the refined ECS model in the design problem.

3.1.2 Ice Protection System (IPS)

The IPS prevents the wing or engine nacelle from forming ice, which causes a reduction in aerodynamic performance. There are several kinds of IPS; one is a thermal method which uses the high temperature bleed air or electric heating. Other methods include a chemical method using de-icing liquid and a mechanical method using bootstraps with air pressure. In this paper, the thermal method is considered for wing ice protection.

The thermal method is described in reference [12]. The necessary power of the IPS is obtained from the required heat value per unit area $\dot{q}_{ps}$. It is calculated by summing the sensible heat $\dot{q}_{sens}$, convective cooling $\dot{q}_{conv}$, evaporative cooling $\dot{q}_{evap}$, kinetic heating $\dot{q}_{KE}$ and aerodynamic heating $\dot{q}_{aero}$ as shown in Eq. (3.5)

$$\dot{q}_{ps} = \dot{q}_{sens} + \dot{q}_{conv} + \dot{q}_{evap} - \dot{q}_{KE} - \dot{q}_{aero} \quad (3.5)$$

Details of each term are described in [2].

The IPS is only used when the altitude is between 8,000 ft and 12,000 ft, because super-cooled water droplets exist in such altitudes.

3.1.3 Hydraulic System

A hydraulic system is used for the operation of the control surfaces and landing gear. The hydraulic system is driven by the engine shaft power. Equation (3.6) describes the necessary power of the hydraulic system:

$$P_{hydr} = k \cdot \frac{\dot{m} \cdot P_l}{600 \cdot \eta_1 \cdot \eta_2} \text{ [kW]} \quad (3.6)$$

where $\dot{m}$ [l/min] is the flow rate of the hydraulic pump, P_l [bar] is load pressure, k is the ratio between the maximum output and the average output of the hydraulic system, η_1 is pump efficiency and η_2 is the efficiency coefficient about pipe pressure loss. Details of each parameter are described in [2].

3.1.4 Electric System

Various systems such as the flight control system, sensors or galley are driven by the electric system. The necessary power for the electric system is calculated based on the data of the electric system of DC-10 in [13]. The necessary power of other electric systems such as cabin lighting or gallery is assumed to be proportional to the number of passengers. Flight control is proportional to the main wing area and necessary power for the toilet is proportional to the number of toilets [2].

3.1.5 Engine Accessory

The engine accessory is composed of the fuel pump, lubricating pump and alternator. Compared to the fuel pump, the necessary power for the lubricating pump and alternator is small. Therefore, only the fuel pump is considered in this paper. In [2], the necessary power of the fuel pump used in B777 was assumed as 55 [kW] per one engine. In this paper, the same value is used.

3.1.6 Weight of Secondary Power Systems

The total weight of aircraft secondary power systems including furnishing is estimated using Eq. (3.7) [14].

$$W_{sys} = k \cdot W_{TO} \ \text{[lb]} \qquad (3.7)$$

where k is 0.14 for the short-haul transport, 0.11 for the medium-haul transport and 0.08 for the long-haul transport. When the More Electric System or Laminar Flow Control System is applied, the weight penalty of these systems is added to the weight of the conventional system in Eq. (3.7). Details of the weight penalty are described in the following sections.

3.2 More Electric System

More Electric System (MES) is a system that replaces the conventional bleed system with an electric system, thus sometimes is expressed as the No Bleed System. In this paper, we consider the electric ECS as one of MES.

Necessary power of the Bleed ECS is set to be $4.158 \cdot 10^{-3}$ [kg/s] per passenger as described in section 3.1.1 and More Electric ECS is assumed to be 1.2[kW] per passenger [15]. Therefore, the necessary power of the More Electric ECS is calculated by multiplying the ratio of these values by the bleed air flow $\dot{m}_{bleed}$ obtained in Eq. (3.4).

Based on reference [2], the necessary ram air is $0.5\dot{m}_{bleed}$ for the pre-cooler and $3.0\dot{m}_{bleed}$ for the heat exchanger in the conventional ECS. In the more electric ECS, the pre-cooler is not necessary. However, the ram air needs to supply the additional air to the system and the amount is the same as $\dot{m}_{bleed}$. Therefore, the ram air for the More Electric ECS is set to be $4.0\dot{m}_{bleed}$.

Moreover, there is a weight penalty in the More Electric ECS due to the change of the system configuration. According to [16], the weight change, if the More Electric ECS is applied to B767, is estimated to be 210 lb. Therefore, the weight penalty of More Electric ECS is calculated as Eq. (3.8) [2].

$$\Delta W_{sys} = 210 \cdot \frac{W_{TO}}{315{,}000} \ \text{[lb]} \qquad (3.8)$$

4. Laminar Flow Control

Laminar flow control has been attracting attention as a technology for realizing fuel reduction by reducing the friction drag on the wing. The boundary layer transition can be delayed by adequately changing the pressure gradient along the flow direction. This is the principle of the laminar flow control.

In this chapter, the overview of the Natural Laminar Flow (NLF) and Hybrid Laminar Flow Control (HLFC) is described based on [17], and the laminar flow control model applied here is explained.

4.1 Natural Laminar Flow (NLF)

The pressure gradient over the wing is dependent on the wing configuration and the boundary layer transition is delayed by adequately designing the wing configuration. Such a technique is called a Natural Laminar Flow (NLF).

For the case of the sweptback wing, in addition to the flow instability observed in the

two dimensional flow (called Tollmien-Schlichting or TS instability), the instability originating from the cross-flow component (called cross-flow or CF instability) is known to be the principle factor of the instabilities.

In reference [17], the occurrence criteria of CF instability is described using the relationship between the sweepback angle and Reynolds number, as shown in Figure 4.1. The solid line indicates the instability limit when the CF instability is observed for the Natural Laminar Flow. The left side of this curve corresponds to the stabilized area. This figure indicates that, as the sweepback angle increases, the Reynolds number decreases when instability occurs.

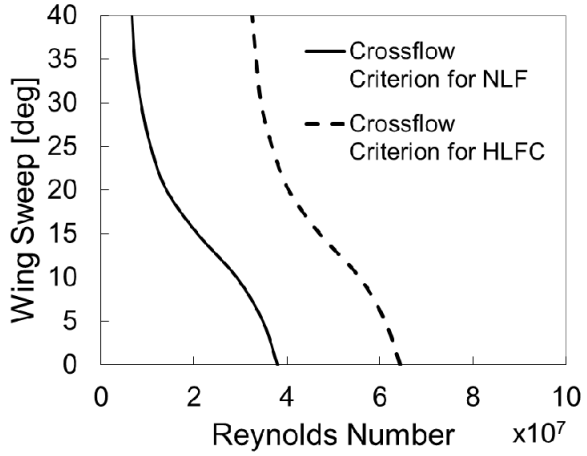

Figure 4.1 Criterion of the CF instability [17]

4.2 Hybrid Laminar Flow Control (HLFC)

The second way for the laminar flow control, is to reduce the velocity component normal to the wall. This is attained by boundary-layer suction through small holes installed over the airfoil surface. The Hybrid Laminar Flow Control (HLFC) applies this boundary-layer suction system near the leading edge of the wing. The NLF design is also applied downstream of the boundary-layer suction system so that the optimum laminar flow control is expected [17]. Figure 4.1 indicates that CF instability is avoided until a higher Reynolds number or a higher sweepback angle by applying HLFC rather than NLF.

The HLFC is operated by the suction pump. Reference [18] conducted a flight test of the boundary-layer suction system. According to the data in [18], the minimum suction flow rate Q of the pump when the laminar flow can be maintained is empirically expressed by Eq. (4.1).

$$Q = 1.1 \cdot A \cdot \frac{U_\infty}{\sqrt{Re}} \text{ [kg/s]} \qquad (4.1)$$

where A is a wetted area [m^2], U_∞ is a uniform flow velocity [m/s] and Re is a Reynolds number based on the mean aerodynamic chord. Based on [19], the necessary power P_{pump} to operate the pump is expressed by Eq. (4.2).

$$P_{pump} = 56.1 \cdot Q \text{ [kW]} \qquad (4.2)$$

Reference [4] applied the flight test results of [19] to Eqs. (4.1) and (4.2), and validated these empirical relationships.

Reference [4] assumed that the weight penalty ΔW_{HLFC} due to the additional HLFC system is 150% of the ECS weight W_{ECS} based on [20] and [21].

$$\Delta W_{HLFC} = 1.5 W_{ECS} \qquad (4.3)$$

The W_{ECS} is estimated from Eq. (4.4), which is obtained by linearly interpolating the data of the existing aircraft (DC-9, MD-80 and DC-10) in [22].

$$\begin{aligned} W_{ECS} &= W_{api} - W_{IPS} \\ W_{api} &= 0.0955 V_{pax} + 1344 \\ W_{IPS} &= (-0.0022 b \\ &\quad + 0.4984) W_{api} \end{aligned} \qquad (4.4)$$

where W_{api} is a total weight of ECS and IPS [lb], V_{pax} is the cabin volume [ft^3], W_{IPS} is IPS weight [lb] and b is a span length [ft].

4.3 Application of the Laminar Flow Control to the Conceptual Design

The effect of the LFC is considered in the conceptual design by applying the following simple estimation criteria based on [17]. Transition based on TS instability is assumed to occur at 50% of local chord length of the wing. The location of CF instability is estimated based on Fig. 4.1. Among the transition locations estimated by the above two criteria, the chord-wise position located close to the leading edge is selected as the actual transition point at each span-wise position. Thus, the total laminar flow area over the surface of the main wing is calculated and laminar area ratio is obtained by dividing the wing's wetted area. Hereafter, this ratio is referred to as Laminar Ratio.

Figure 4.2 indicates the estimated transition location measured from the leading-edge for the B777-200 main wing during cruise. Transition point due to TS instability and transition point due to CF instability when NLF or HLFC is applied are indicated in this figure. As for NLF, transition is caused by CF instability, except near the wing tip area, because of the reduced Reynolds number. As for HLFC, transition is caused by TS instability for the whole span range. Laminar Ratio is calculated based on Fig. 4.2. When NLF is applied, Laminar Ratio is 0.21, and when HLFC is applied, it is 0.50. According to [20], it is suggested that the transition point is about 50% of the local chord length when HLFC is applied.

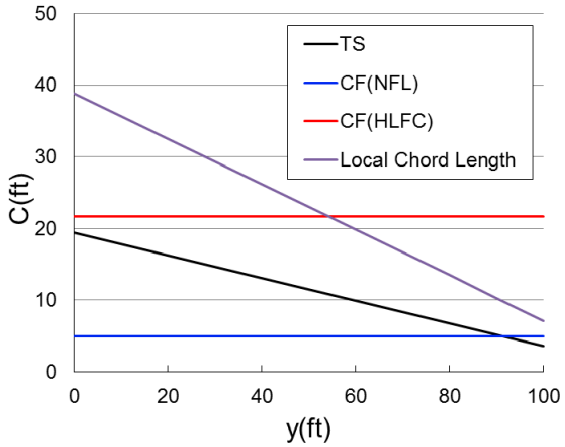

Figure 4.2 Estimated Transition Location measured from the Leading Edge of the Main Wing (B777-200)

5. Engine Analysis

In the trajectory calculation, we need to know the engine performance in the wide range of altitudes, Mach number and thrust rating. Moreover, the secondary power system affects the engine performance by extracting bleed air and power off-take. Thus, a detailed engine-performance calculation is required to consider the secondary power system in the conceptual design. In this paper, engine performances are obtained by the commercial engine performance analysis software GasTurb12 [23].

GasTurb has a feature called Off-Design that can obtain the engine performance of the outside of the design point. As an example, Figure 5.1 shows the relationship between thrust, altitude and specific fuel consumption sfc at a cruise Mach number of M0.84 for the Trent877 engine. From this figure, it can be seen that thrust and altitude have a great impact on sfc. Figure 5.2 shows the relationship between the power off-take PWX, bleed air and sfc. From this figure, it is said that the secondary power off-take affects sfc. When the amount of power off-take increases, sfc increases.

In this paper, we also use these data to estimate the effect of the secondary power system in the conceptual design.

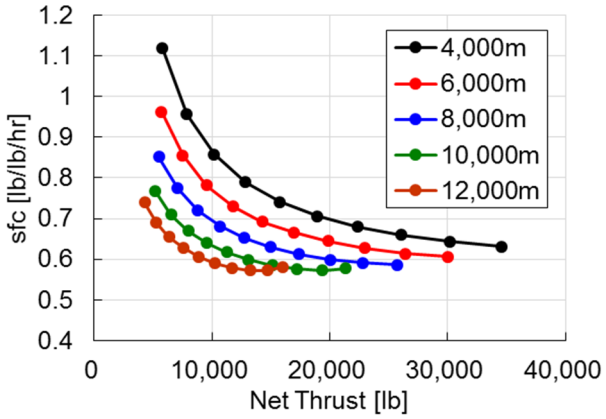

Figure 5.1 Relationship between Thrust, Altitude and Specific Fuel Consumption (M0.84)

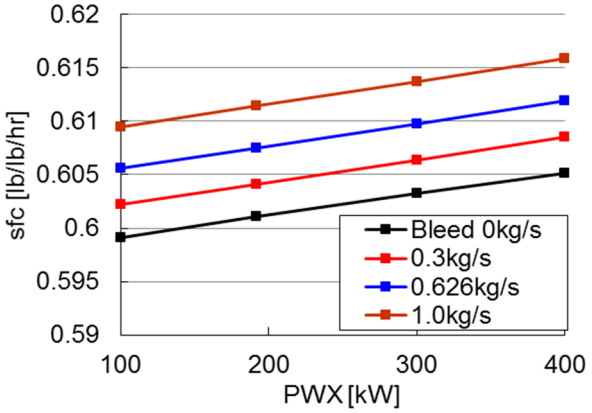

Figure 5.2 Relationship between Power Off-take and Specific Fuel Consumption

6. Conceptual Design Method

In this chapter, we apply the trajectory calculation to the conceptual design method considering the secondary power systems based on [2] and [3]. The flowchart of the design method proposed in this paper is shown in Figure 6.1. The orange-colored sections are the weight

estimation module considering the aircraft trajectory and the secondary power systems.

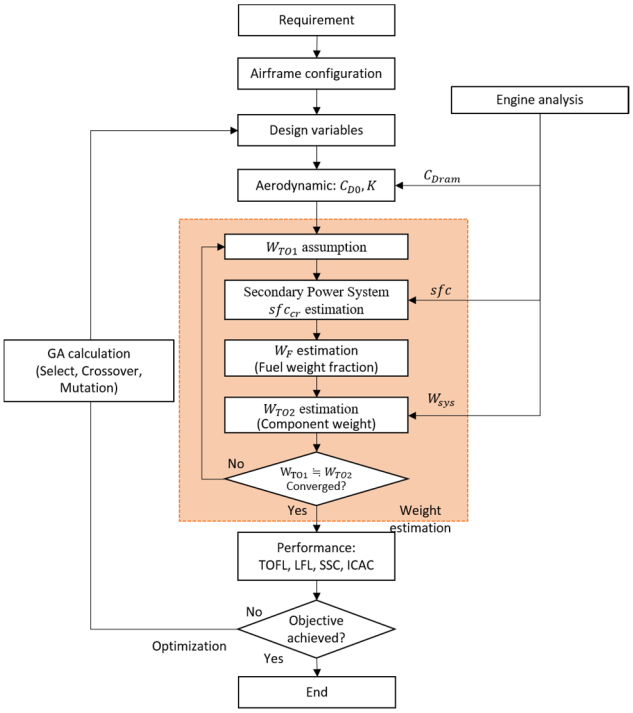

Figure 6.1 Flowchart of the Conceptual Design

6.1 Weight Estimation Module Considering Aircraft trajectory

In the weight estimation module, the trajectory calculation is used to estimate the fuel weight. First, we assume the take-off weight W_{TO1} and set it as the initial weight. The trajectory calculation is conducted and fuel weight is estimated. The trajectory calculation includes the aerodynamic and engine performance calculations. Then, we calculate the operating empty weight using the conventional weight estimation method [24] and conduct iterative calculations until the take-off weight is converged.

Since the aircraft dynamic model described in Eq. (2.1) is a simplified one, it is difficult to calculate flight phases such as take-off, landing or taxi. Therefore, the trajectory calculation begins in the climb phase and terminates in the descent phase. Other flight phases are calculated using the fuel fraction method [24].

6.2 Minimum Fuel Optimization Problem

In Chapter 7, the main discussion of this paper will be made. The reference aircraft selected for this discussion is B777-200. The reference engine is Trent877, as shown in Chapter 5. The objective function for this design problem is the fuel weight W_F and a single optimization problem to minimize W_F was performed. The design requirements and constraints are shown in Tables 6.1 and 6.2. The design constraints are take-off field length $TOFL$, landing field length LFL, climb gradient requirement at second segment CGR, initial cruise altitude capability $ICAC$, horizontal wing volume V_h, vertical wing volume V_v and center of gravity location $C.G.$ The design variables are main wing area S, horizontal wing area S_h, vertical wing area S_v, the distance between the nose and the leading edge of the main wing $APEX_w$ (divided by the fuselage length). The design variable ranges are shown in Table 6.3. As an optimization tool, the Genetic Algorithm (GA), NSGA-II [25] is used. The calculation condition of GA is shown in Table 6.4.

Table 6.1 Design Requirements (B777-200) [10]

Passenger	305
Altitude [ft]	37,000
Mach No.	0.84
Range [nm]	5,210

Table 6.2 Design Constraints (B777-200)

$TOFL$ [ft] [10]	$\leq$ 8,450
LFL [ft] [10]	$\leq$ 5,150
CGR [%]	$\geq$ 2.4
$ICAC$ [ft/min]	$\geq$ 300
V_h	$\geq$ 0.9
V_v	$\geq$ 0.085
$C.G.$	$\cong$ 25%MAC

Table 6.3 Design Variables (B777-200)

S [ft^2]	$4{,}000 \leq S \leq 6{,}000$
S_h [ft^2]	$900 \leq S_h \leq 1{,}400$
S_v [ft^2]	$800 \leq S_v \leq 1{,}300$
$APEX_w$	$0.2 \leq APEX_w \leq 0.5$

Table 6.4 GA condition

Population	100
Generation	100
Crossover rate	0.8
Mutation rate	0.03
Objective function	W_F

6.3 Accuracy Verification of the Design Method

Before applying the proposed design method to the main design problem, we applied this method to the following design problem to confirm the accuracy of this method. In addition to B777-200, we selected B737-700 as a reference aircraft. The reference engine for B737-300 is CFM56-7B24 and its performance was estimated using the method in Chapter 5. The design requirements and constraints for B737-700 are shown in Tables 6.5 and 6.6. To make this validation simplified, the aircraft configurations, including the design variables, were fixed in the same way as the existing aircraft obtained from [10].

The results of B737-700 are shown in Table 6.7 and those of B777-200 are shown in Table 6.8. The estimated values of B737-700 indicate close agreements with those of the existing aircraft. On the other hand, in B777-200, the maximum take-off weight W_{TO} is slightly heavier than that of the existing aircraft, and its difference is about 3%.

Table 6.5 Design Requirements (B737-700) [10]

Passenger	125
Altitude [ft]	36,000
Mach No.	0.785
Range [nm]	3,240

Table 6.6 Design Constraints (B737-700)*

TOFL [ft] [10]	≤ 5,400
LFL [ft] [10]	≤ 4,800

* other design constraints are the same as for B777-200 (Table 6.2).

Table 6.7 Design Results (B737-700)

	Result	B737-700 [10]
W_{TO}[lb]	155,000	155,000
W_{OE}[lb]	84,200	84,100
W_F[lb]	45,800	N/A
T_{TO}[lb]	48,100	49,000

Table 6.8 Design Results (B777-200)

	Result	B777-200 [10]
W_{TO}[lb]	558,000	545,000
W_{OE}[lb]	293,000	302,000
W_F[lb]	205,000	N/A
T_{TO}[lb]	157,000	154,000

7. Application to the Design Problem

In this chapter, we describe the result of applying the proposed design method to the design problem. Two advanced aircraft systems, More Electric System and Laminar Flow Control, are considered. The reference aircraft is B777-200, as is described in Section 6.2.

7.1 Effect of More Electric System

In this section, we consider the results of MES. The results obtained by the present method are shown in Table 7.1. Those obtained by the method in [2] and [3], without considering aircraft trajectory, are shown in Table 7.2. Figure 7.1 shows the rate of change in each value that indicates how replacing bleed air with MES influences the design results when compared with bleed air systems. The results obtained by trajectory calculation are shown in Figures 7.2 to 7.7. The black lines are the results of the conventional bleed system and the red lines are those of the MES in these figures, except Figs. 7.4 and 7.5.

Figure 7.2 shows the aircraft trajectory considered in this calculation. During the cruise, the step climb is considered. Figure 7.3 shows the specific fuel consumption sfc during the cruise. Figures 7.4 and 7.5 show the bleed air mass flow rate and power off-take of the ECS at the climb phase. The dotted line is the result of the estimation model used in [2] and [3], and the solid line is that of the present refined ECS model. Both the bleed air mass flow and the necessary power estimated in the present model are larger than those of the conventional model (dotted line). This means the effect of MES becomes larger in the climb and descent phases. Next, we verify the aerodynamic performance during the cruise. Figure 7.6 shows the drag coefficient and Figure 7.7 shows the lift to drag ratio during the cruise. The drag coefficient increases for the

MES case. The drag increase is caused by the additional ram air of MES. Moreover, lift to drag ratio also decreases for MES. In this way, the MES indicates poor aerodynamic performance compared to the bleed system. However, Figure 7.1 indicates that the fuel weight W_F decreases by nearly 1% by applying the MES. This is thought to be brought about by the effect of reduction of sfc, which exceeds the penalty of aerodynamic performance in the present model. In addition, the reduction of W_F reduces the maximum take-off weight W_{TO} and operating empty weight W_{OE}.

Next, we compare the present results and those based on the method [2] and [3] without trajectory consideration. Figure 7.1 indicates that the difference between them is small. However, as shown above, aircraft trajectory consideration enabled the details of the aerodynamic and performance characteristics during cruise to be comprehended.

Table 7.1 Results based on the Present Method

	Bleed	MES
W_{TO}[lb]	560,000	557,000
W_{OE}[lb]	294,000	293,000
W_F[lb]	206,000	205,000
T_{TO}[lb]	158,000	157,000
S[ft^2]	4,620	4,590
S_h[ft^2]	1,170	1,150
sfc[lb/lb/hr]*	0.595	0.590
W/S [lb/ft^2]	121	121
T/W	0.281	0.282

* averaged value during cruise

Table 7.2 Results based on the Method [2] and [3] without Aircraft Trajectory Consideration

	Bleed	MES
W_{TO}[lb]	558,000	556,000
W_{OE}[lb]	293,000	292,000
W_F[lb]	206,000	204,000
T_{TO}[lb]	157,000	157,000
S[ft^2]	4,600	4,580
S_h[ft^2]	1,160	1,160
sfc[lb/lb/hr]*	0.590	0.587

* averaged value during cruise

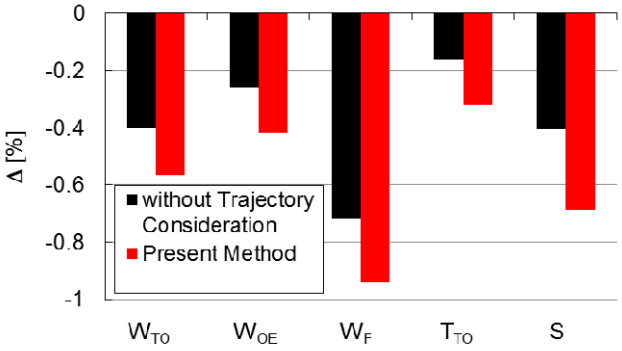

Figure 7.1 Effects of More Electric System

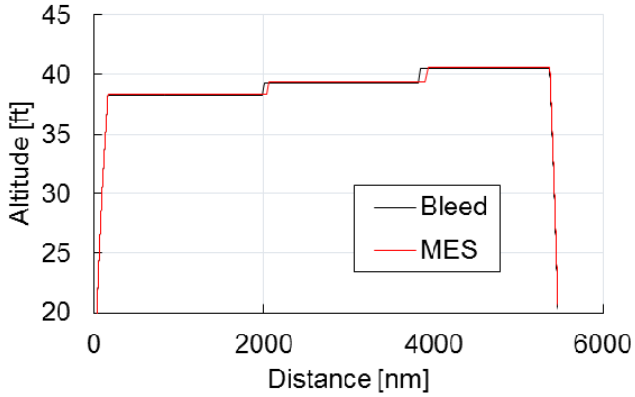

Figure 7.2 Aircraft Trajectory

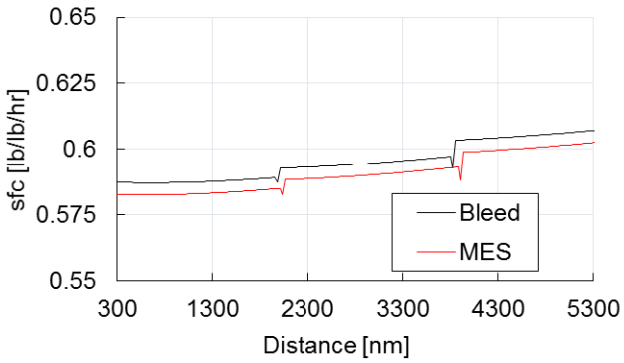

Figure 7.3 Specific Fuel Consumption during Cruise

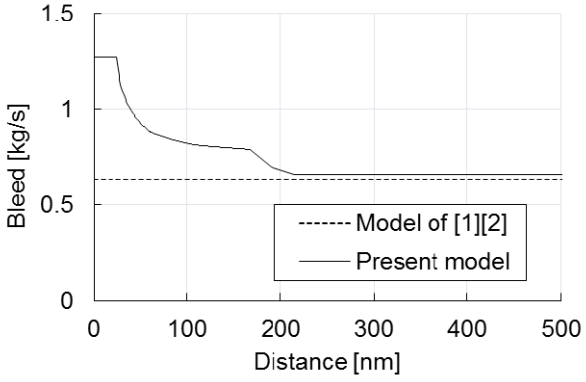

Figure 7.4 ECS Bleed Air Mass Flow $\dot{m}_{bleed}$ During Climb

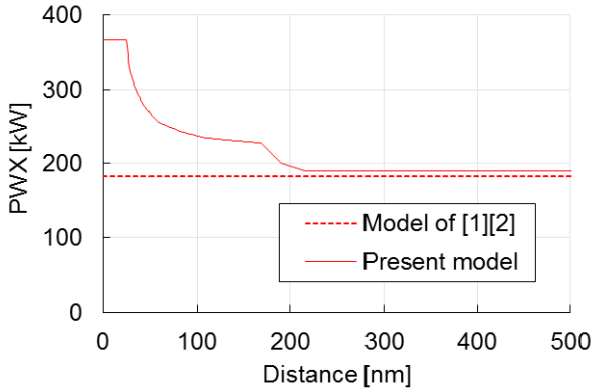

Figure 7.5 ECS Power Off-take during Climb

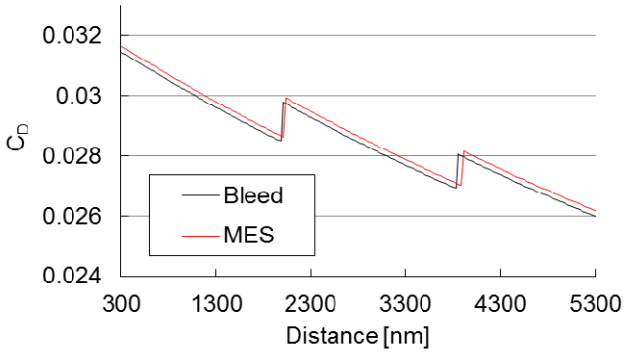

Figure 7.6 Drag Coefficient during Cruise

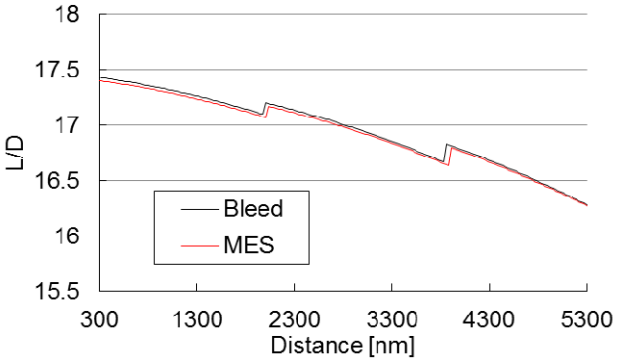

Figure 7.7 Lift to Drag Ratio during Cruise

7.2 Effect of Laminar Flow Control

In this section, we consider the effect of laminar flow control. Three types of aircraft are considered here, which are an aircraft which does not apply the Laminar Flow Control (No LFC), one which applies the Natural Laminar Flow (NLF), and one which applies the Hybrid Laminar Flow Control (HLFC). HLFC is applied only over the upper surface of the main wing.

Table 7.3 shows the result of the present method. Figure 7.8 shows the rate of change in each value that indicates how applying the NLF and the HLFC influences the design results when compared with the No LFC results. Figures 7.9 to 7.14 show all the results obtained by the present method. The black lines indicate the results of No LFC, the green lines indicate those of NLF, and the red lines those of HLFC. According to [6], the laminar ratio of the main wing for the transport aircraft is 0.1 to 0.15. Thus, the laminar ratio of No LFC was assumed to be 0.15.

The aircraft trajectory is shown in Figure 7.9. Figure 7.10 shows the parasite drag coefficient C_{D0} during the cruise. This figure indicates that C_{D0} become the smallest for the HLFC case and the second smallest for the NLF case. The average value of C_{D0} of HLFC is about 6% smaller than that of No LFC. Figure 7.11 indicates that the lift-to-drag ratio L/D becomes the maximum for the HLFC case. On the other hand, sfc of NLF and HLFC during the cruise are larger than that of No LFC (Fig. 7.12). This is caused by the decrease in necessary thrust during the cruise T(Fig. 7.13) and consequently sfc is increased (please refer to Fig. 5.1). In this way, sfc reaches maximum in HLFC. However, the fuel flow during the cruise becomes the smallest in HLFC, as shown in Fig. 7.14, because T is decreased. As a result, W_F of HLFC is smaller than that of NLF, as shown in Table 7.3 and Fig. 7.8. HLFC indicated the best performance. The operating empty weight$W_{OE}$is decreased in NLF compared to No LFC, however, it is increased in HLFC because of the system weight penalty. Thus, the minimum W_{TO} was obtained in the case of NLF.

Table 7.3 Results of the Present Method

	No LFC	NLF	HLFC
W_{TO}[lb]	560,000	553,000	557,000
W_{OE}[lb]	294,000	290,000	296,000
W_F[lb]	206,000	203,000	201,000
T_{TO}[lb]	158,000	154,000	151,000
S[ft^2]	4,620	4,560	4,600
S_h[ft^2]	1,170	1,150	1,160
Laminar Ratio*	0.15	0.21	0.35
W/S [lb/ft^2]	121	121	121
T/W	0.281	0.279	0.272

* averaged value of upper and lower surfaces

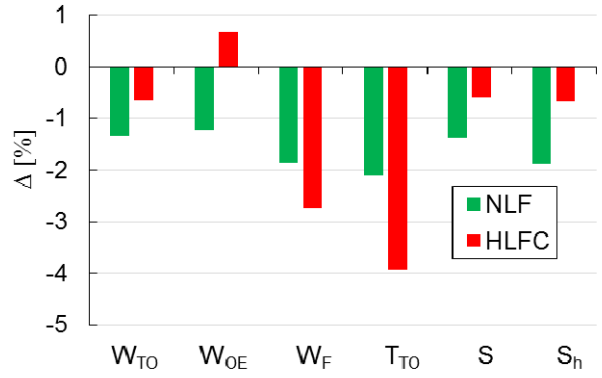

Figure 7.8 Effect of Laminar Flow Control

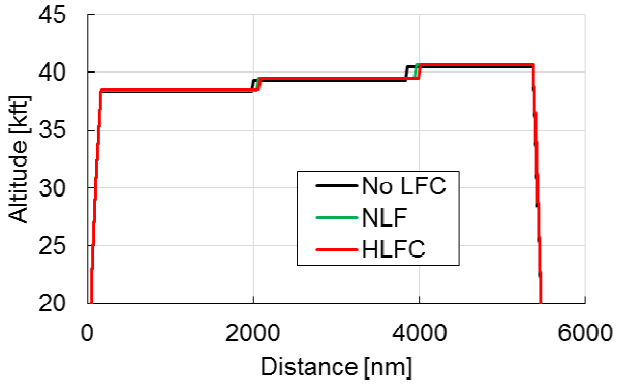

Figure 7.9 Aircraft Trajectory

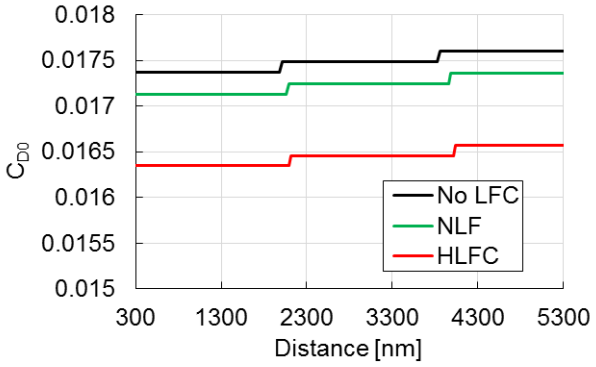

Figure 7.10 Parasite Drag Coefficient during Cruise

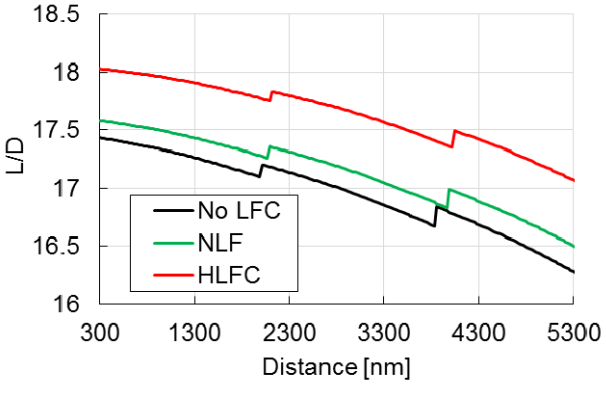

Figure 7.11 Lift to Drag Coefficient during Cruise

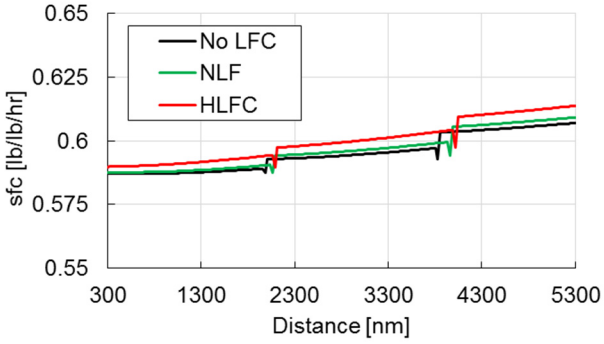

Figure 7.12 Specific Fuel Consumption during Cruise

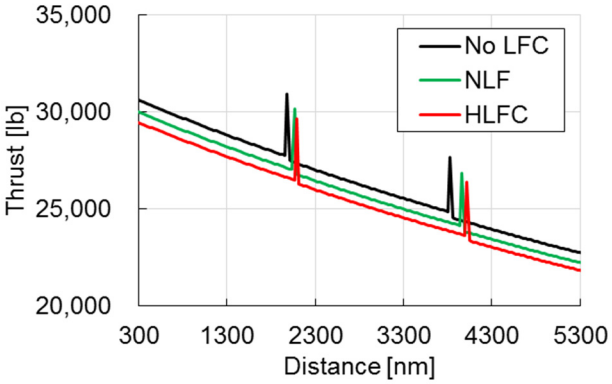

Figure 7.13 Necessary Thrust during Cruise

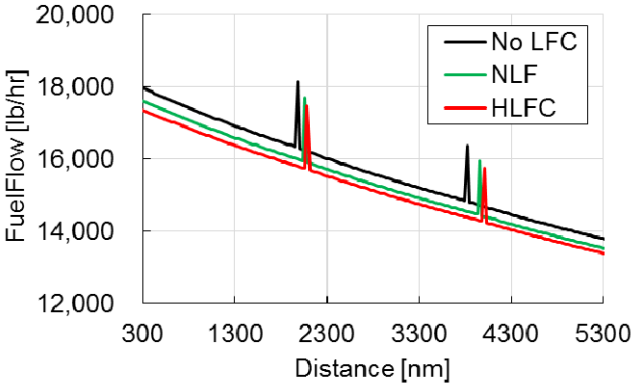

Figure 7.14 Fuel Flow during Cruise

As described in Section 6.3, the estimated maximum take-off weight by use of the present method indicated about a 3% error. Since the present method is based on the theoretical and semi-empirical models for the aircraft performance, aircraft weight and secondary power systems, these models contain uncertainties. Thus, the numerical values in these sections should be treated with caution. To discuss this matter, [2] and [4] conducted a sensitivity analysis. Here, a similar analysis is made for the HLFC case. Figure 7.15 indicates

the changes in fuel weight W_F, when the necessary power of the suction pump P_{pump} (Eq. (4.2)), HLFC system weight penalty ΔW_{HLFC} (Eq. (4.3)) and the Laminar Ratio (Section 4.3) are changed by ±20%, independently. This figure shows that the changes of W_F are almost proportional to the changes of these three parameters. It also shows that the amount of change in W_F is about 0.1%, 0.6% and 2% for P_{pump}, ΔW_{HLFC} and Laminar Ratio, respectively, when these estimated values are changed by 20%. This indicates that among three parameters considered here, the Laminar Ratio estimation model has the largest effect on the design results and the necessary power model of the pump has little effect on them, which are the similar conclusions discussed in [4].

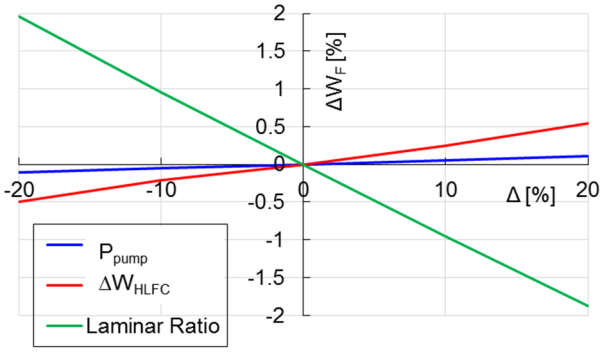

Figure 7.15 Effects on Fuel Weight by the HLFC models

8. Conclusions

The conceptual design method considering the advanced aircraft systems and aircraft trajectory was proposed in this paper. The proposed method was applied to design problems of heavy aircraft (reference aircraft: B777-200), and the effects of the More Electric System and Laminar Flow Control were considered. As a result, the following conclusions were obtained.

- Consideration of aircraft trajectory made it possible to comprehend the overall trend of aerodynamic performance and fuel consumption during the cruise when advanced aircraft systems were considered.
- Fuel weight W_F can be reduced by considering the optimum cruise altitude.

From the results of the More Electric System (MES)

- According to the MES model used here, while there are drag increases and weight penalties in the MES, the specific fuel consumption sfc, and hence W_F, can be reduced, when the more electric environmental control system (ECS) is applied.
- The necessary powers of ECS during the climb and descent are larger than during cruise. Thus, the effect of the MES increases during the climb and descent phases.

From the results of the Laminar Flow Control (LFC)

- According to the LFC model used here, by applying the natural laminar flow (NLF) or the Hybrid Laminar Flow Control (HLFC), the lift/drag ratio L/D increases. The specific fuel consumption sfc during cruise is increased both for the NLF and HLFC cases because the necessary thrust is decreased by the improvement of aerodynamic performance. However, the fuel flow during the cruise is decreased.
- Due to the decrease in the fuel flow, W_F is decreased both for the NLF and HLFC cases. The maximum take-off weight W_{TO} is also decreased. Because of the system weight penalty of HLFC, W_{TO} becomes the smallest for the NLF case.

The conceptual design method and the aircraft system models used in this paper contain certain amounts of error. Thus, the numerical values obtained here should be treated with caution. However, the present method is useful to comprehend the effect of the advanced systems upon the aircraft conceptual design results.

References

[1] Shibata, K., and Rinoie, K.: Conceptual Design Method Considering Aircraft Secondary Power Systems Effect on Aircraft Performance, Aerospace Technology, Vol.14, 2015, pp.23-32 (in Japanese).

[2] Shibata, K., Maedomari, T., Rinoie, K., Morioka, N. and Oyori, H.: Aircraft Secondary Power System Integration into Conceptual Design and Its Application to More Electric System, SAE 2014

Aerospace Systems and Technology Conference, Cincinnati, Paper No. 2014-01-2199, 2014.
[3] Shibata, K., Maedomari, T., Rinoie, K., Morioka, N., and Oyori, H.: Conceptual Design Method Considering Aircraft Secondary Power System and Its Application to More Electric System, 52th Aircraft Symposium, Takamatsu, 2014 (in Japanese).
[4] Shibata, K., Rinoie, K.: Conceptual Design Method Considering Laminar Flow Control System Effect on Aircraft Performance, 52th Aircraft Symposium, Takamatsu, 2014 (in Japanese).
[5] Rinoie, K.: Aircraft Conceptual Design –from Light Aircraft to Supersonic Transport, Corona Publishing, Tokyo, 2011 (in Japanese).
[6] Raymer, D. P.: Aircraft Design: A Conceptual Approach, AIAA, Washington, 1992.
[7] Shinkafi, A., Lawson, C., Seresinhe, R., Quaglia, D., and Madani, I.: An Intelligent Ice Protection System for Next Generation Aircraft Trajectory Optimisation, 29th Congress of the International Council of the Aeronautical Sciences, ICAS-2014-10.1.2, 2014.
[8] Seresinhe, R., Lawson, C., Shinkafi, A., Quaglia, D., and Madani, I.: Airframe Systems Power Off-take Modelling in More-electric Large Aircraft for Use in Trajectory Optimisation, 29th Congress of the International Council of the Aeronautical Sciences, ICAS 2014-10.1.3, 2014.
[9] Hok, K. Ng., Srindhar, B. andGrabbe, Sh.: Optimizing Aircraft Trajectories with Multiple Cruise Altitudes in the Presence of Winds, Journal of Aerospace Information Systems, Vol.11, No.1, pp.35-47, 2014.
[10] Jackson, P.: Jane's All the World's Aircraft 2011-2012. Janes Information Group, London, 2011.
[11] Martinez, I.: Aircraft Environmental Control, http://webserver.dmt.upm.es/~isidoro/tc3/Aircraft%20ECS.pdf (retrieved on January 29, 2015).
[12] Meier, O. and Scolz, D., http://www.fzt.haw-hamburg.de/pers/Scholz/MOMOZA/MOZART_PUB_DLRK_10-08-31.pdf, (retrieved on April 22, 2013).
[13] Roskam, J.: Airplane Design, Part V, Component Weight Estimation, DARcorporation, Kansas, 1985.
[14] Jenkinson, L. R., Simpkin, P. and Rhodes, D.: Civil Jet Aircraft Design, Arnold, London, 1999.
[15] Barreau, L., Eglem, M. and Heraud, P.: "Anti-condensation Method and Device for an Aircraft," U.S. Patent 0 199 315, Aug. 9, 2012.
[16] Berlowitz, I.: http://jet-engine-lab.technion.ac.il/9aijes/9.All,More Electric Aircraft Engine & Airframe Systems Implementation, Bedek Aviation Group, Aircraft Programs Division, Israel Aerospace Industries, Israel.pdf, (retrieved in December 1,2012).
[17] Lehner, S. and Crossley, W.: Combinatorial Optimization to Include Greener Technologies in a Short-to-medium Range Commercial Aircraft, 26th International Congress of the Aeronautical Sciences, ICAS-2008-4.10.2.
[18] Maddalon, D. V., Collier, F. S., Montoya. L. C., Land, C. K.: Transition Flight Experiments on a Swept Wing with Suction. AIAA 20th Fluid Dynamics, Plasma Dynamics and Lasers Conference, AIAA89-1893, New York, 1989.
[19] Schmitt, V., Archamband, J. P., Hortstmann, K. H., Quast, A.: Hybrid Laminar Fin Investigations. ONERA/DLR Aerospace Symposium, Paris, 1999.
[20] Joslin, R. D.: Overview of Laminar Flow Control, NASA TP-1998-208705, 1998.
[21] Arcara, P. C. Jr, Bartlett, D. W. and McCullers, L. A.: Analysis for the Application oh Hybrid Laminar Flow Control to a Long- Range Subsonic Transport Aircraft. Aerospace Technology Conference and Exposition, Long Beach, California, SAE Paper 912113, 1991.
[22] Roskam, J. : Airplane Design Part V: Component Weight Estimation. DARcorporation, Kansas, 1999.
[23] Kurzke, J.: GasTurb12 Manual, 2012.
[24] Roskam, J.: Airplane Design, Part I, Preliminary Sizing of Airplanes, DARcorporation, Kansas, 1985.
[25] Deb, K., Pratap, A., Agarwal, S. and Meyarivan, T.: A Fast and Elitist Multiobjective Genetic Algorithm: NSGA-II, IEEE Transactions on Evolutionary Computation, Vol. 6, No. 2, April 2002.

Copyright Statement